Atmospheric
Chemistry
and Physics

Open Access

EGU

Supplement of

Representing sub-grid scale variations in nitrogen deposition associated with land use in a global Earth system model: implications for present and future nitrogen deposition fluxes over North America

Fabien Paulot et al.

Correspondence to: Fabien Paulot (fabien.paulot@noaa.gov)
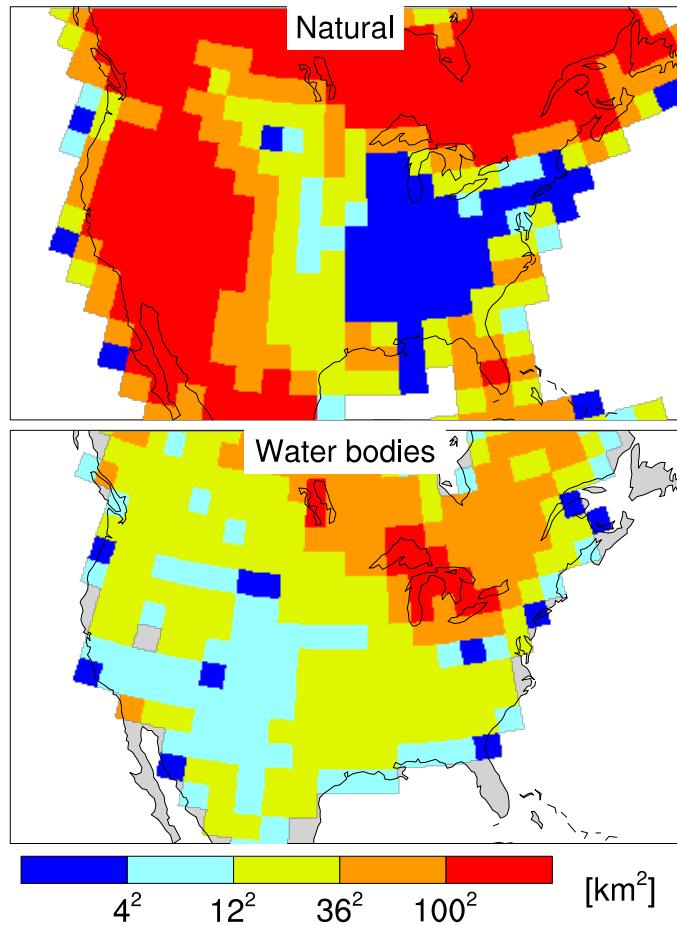
Figure S1: Average area covered by natural vegetation and water bodies from 2008-2010.

ΔLAI

[unitless]

-2.5 -2.25 -2 -1.75 -1.5 -1 -0.5

Δvegetation height

[m]

-18 -16 -14 -12 -10 -8 -6 -4 -2
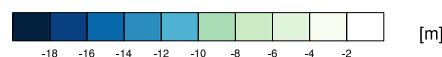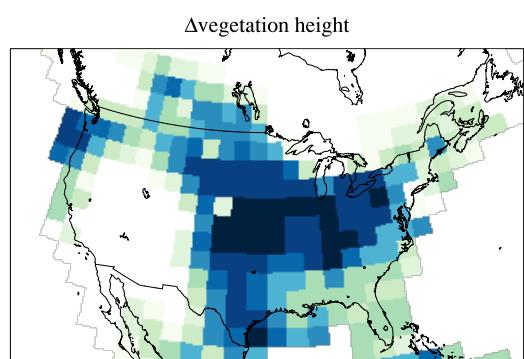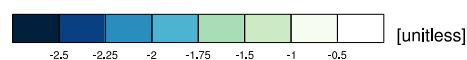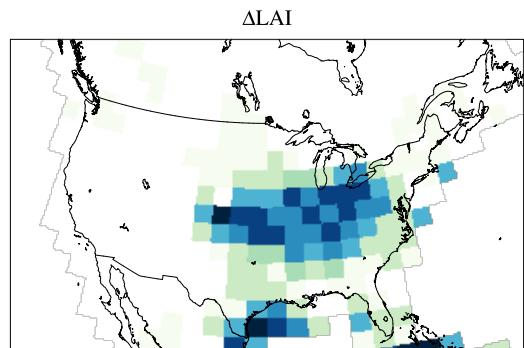
Figure S2: Average change in LAI and vegetation height associated with anthropogenic land-use change from 2008 to 2010.

Sensitivity of $v_d(\mathrm{HNO_3})$ and $v_d(\mathrm{NH_3})$ to surface properties

$\mathrm{NH_3}$ and $\mathrm{HNO_3}$ are the most important contributors to N dry deposition in the US(Zhang et al., 2012) and we focus here on the impact of surface properties on $v_d(\mathrm{NH_3})$ and $v_d(\mathrm{HNO_3})$. Fig. S3 shows the simulated $v_d(\mathrm{HNO_3})$ and $v_d(\mathrm{NH_3})$ over natural vegetation (green solid line) in two grid cells located in North America: (35°N, -83.75°W) and (51°N, -116.25°W). These grid boxes encompass the Great Smoky Mountains National Park (GSM) in the US and the Banff National Park in Canada. Natural vegetation is comprised of deciduous forest at GSM and coniferous forest at Banff with similar vegetation height ($\sim 20m$) and summer LAI (5–6).

Simulated $v_d(\mathrm{HNO_3})$ is 50% faster at Banff than GSM. Such enhancement over coniferous forests is consistent with observations (Meyers et al., 1989; Sievering et al., 2001; Pryor and Klemm, 2004) and reflects the lower laminar resistance associated with needles relative to deciduous leaves (eq. 1). In contrast, the widely used parameterization of Hicks et al. (1987) (Hicks et al., 1987) suggests a negligible impact of species changes on $v_d(\mathrm{HNO_3})$.

Unlike $\mathrm{HNO_3}$, $R_{sf,v}(\mathrm{NH_3})$ can be large, which exacerbates the sensitivity of $v_d(\mathrm{NH_3})$ to surface properties. This results in a more pronounced seasonality for $v_d(\mathrm{NH_3})$ than $v_d(\mathrm{HNO_3})$, with a maximum in summer and a large impact of acidity and canopy wetness. For instance, $v_d(\mathrm{NH_3})$ in the fall can be twice as large at Banff when canopy wetness is accounted for. At GSM and Banff, the dry deposition of acids is predicted to exceed that of $\mathrm{NH_x}$ and co-deposition is simulated to increase $v_d(\mathrm{NH_3})$ by up to 100%.

Fig. S3 also shows that $v_d(\mathrm{HNO_3})$ and $v_d(\mathrm{NH_3})$ over pasture (magenta) and cropland (red) at GSM are slower than over the collocated forest. For $\mathrm{HNO_3}$, this reflects the lower vegetation height, which results in slower $u_\star$ and greater $R_{b,v}$(Hicks, 2006). For $\mathrm{NH_3}$, the lower LAI contributes to the slower $v_d(\mathrm{NH_3})$. The largest reduction relative to natural vegetation is for cropland before and after harvest highlighting the importance of management practices (e.g., grazing intensity, cropping schedule) for N deposition. AM3–LM3 simulates faster $v_d(\mathrm{NH_3})$ over water bodies relative to vegetated surfaces, especially outside of the growing season, but slower $v_d(\mathrm{HNO_3})$. These differences can be attributed to the large effective solubility of $\mathrm{NH_3}$ in freshwater and to the low roughness height of water bodies respectively.
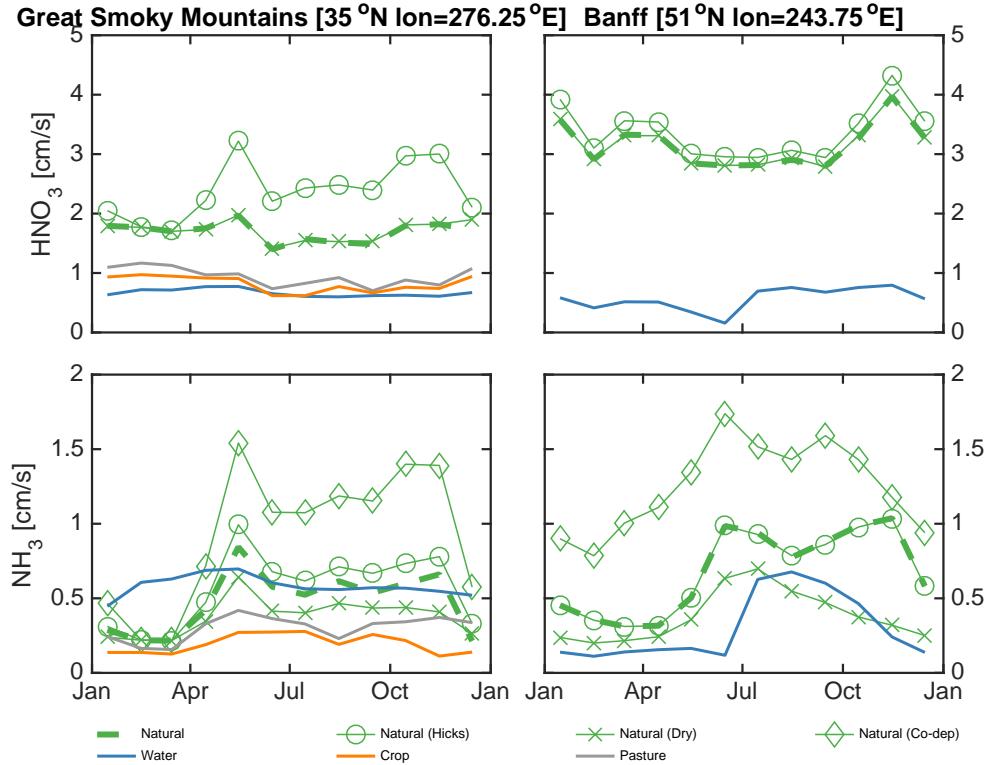
Figure S3: Simulated monthly deposition velocities of HNO_3 and NH_3 for natural vegetation (green), cropland (red), pasture (purple), and water bodies (blue) in the model grid cells that encompass Great Smoky Mountains National Park (GSM, left column) and Banff (right column). The simulated natural vegetation is deciduous tree at GSM and coniferous tree at Banff The green circles show the simulated deposition velocities over natural vegetation when the laminar resistance depends solely on the friction velocity $(u_\star)$ (Hicks et al., 1987), neglecting the impact of leaf width(Jensen and Hummelshøj, 1997). Green stars show the simulated deposition velocity when the canopy is assumed to be dry. The green dash line shows the simulated deposition velocity of NH_3 when $R_{ns}(NH_3)$ is allowed to decrease with increasing acid deposition (co-deposition).
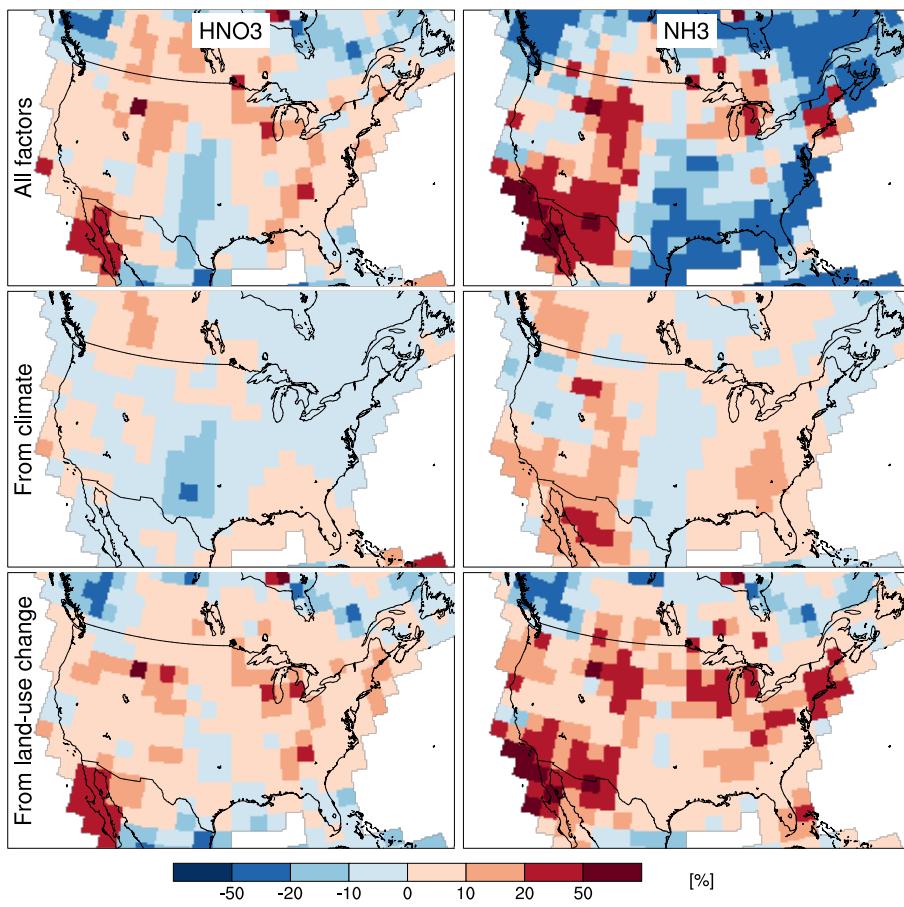
Figure S4: Simulated change in deposition velocity between 2010 and 2050 for HNO_3 and NH_3 (top panel). The contribution of climate change and land-use change to the overall change are shown in the middle and bottom panels respectively.

Table S1: Parameters used for the different LM3 land and vegetation types

	pasture	crop	temperate deciduous	tropical	evergreen	c3 grass	c4 grass	wetland	lake	glacier
$R_{sf,v}(SO_2)$ [a]	1000	1500	2500	2500	2000	1000	1000	1500		
$R_{sf,v}(O_3)$ [a]	4000	4000	4000	4000	4000	4000	4000	4000		
$R_{sf,v}(SO_2, \text{wet})$ [a]	100	100	100	100	100	100	100	100		
$R_{sf,v}(O_3, \text{wet})$ [a]	200	200	400	400	200	200	200	300		
$R_{sf,g}(SO_2)$ [a,b]	200	200	200	100	200	200	200	50	20	70
$R_{sf,g}(O_3)$ [a,b]	200	200	200	100	200	200	200	500	500	2000
$R_{sf,s}(SO_2)$ [c]	1000	1000	1000	1000	1000	1000	1000	1000		
$R_{sf,s}(O_3)$ [d]	4000	4000	4000	4000	4000	4000	4000	4000	4000	4000
lw (cm) [e]	1	5	3	5	0.15	1	1	see note (f)		

[a] resistances from Zhang et al. (2003)

[b] the surface resistance is set to 700 s/m (desert) for vegetated tiles with above ground biomass lower than 0.25 $\mathrm{kg\,m^{-2}}$

[c] from Padro et al. (1993)

[d] assuming $R_{sf,s}(O_3)/R_{sf,s}(SO_2)$ is the same as $R_{sf,v}(O_3)/R_{sf,v}(SO_2)$ in pasture

[e] from Petroff and Zhang (2010)

[f] based on the tile vegetation type

Table S2: Compound specific adjustment

Name	α	β	MW (kg/mol)
H_2O_2 [a,b]	100000	1	0.034
Hydroxyacetone [a]	5	1	0.149
HCOOH [a]	0.056	1	0.045
HNO_3 [a]	100000	1	0.063
IEPOX [a]	20	1	0.118
ISOPNB [a]	7	1	0.147
ISOPND [a]	7	1	0.147
$ISOPNO_3$ [a]	7	1	0.147
ISOPOOH [a]	20	1	0.118
MACRN [a]	7	1	0.149
MACROOH [a]	20	0	0.12
MPAN [c]	0	1	0.147
MVKN [a]	7	1	0.149
N_2O_5 [d]	100000	1	0.063
PAN [c]	0	2	0.121
PROPNN [a]	7	1	0.119

[a] α and β tuned to capture Nguyen et al. (2015) measurements

[b] no adjustment for cold temperature is done following Wesely (1989)

[c] following WU ET AL. (2012)

[d] assumed to follow HNO_3

Table S3: Observations of $v_d(SO_2)$ used in Fig. 4

LM3 tile/vegetation	ID	Reference	Latitude [°N]	Longitude [°E]
Natural/Deciduous				
	D1	Finkelstein et al. (2000)	41.59	-78.77
	D2	Matt et al. (1987)	35.95	-84.28
	D3-4	Neirynck et al. (2011)	51.30	4.52
	D5	Padro (1994)	44.32	-80.93
	D6	Wu et al. (2016)	44.32	-79.93
Natural/Coniferous				
	C1-2	Erisman (1994)	52.08	5.83
	C3	Granat and Richter (1995)	60.90	16.70
Natural/Tropical				
	T1-2	Matsuda et al. (2006)	18.28	99.72
	T3	Tsai et al. (2010)	24.08	121.13
Crop or Pasture/Grass				
	G1	Erisman (1994)	52.13	4.83
	G2-5	Feliciano et al. (2001)	40.70	-8.61
	G6-8	Fowler et al. (1995)	52.82	-1.25
	G9-12	Garland et al. (1974)	52.13	-0.45
	G13-15	Meyers et al. (1998)	40.05	-88.37
	G16	Myles et al. (2012)	35.97	-79.00
	G17-18	Sorimachi et al. (2003)	39.96	116.36

References

Erisman, J. W.: Evaluation of a surface resistance parametrization of sulphur dioxide, Atmos. Environ., 28, 2583–2594, 1994.

Feliciano, M. S., Pio, C. A., and Vermeulen, A. T.: Evaluation of SO_2 dry deposition over short vegetation in Portugal, Atmos. Environ., 35, 3633–3643, 2001.

Finkelstein, P. L., Ellestad, T. G., Clarke, J. F., Meyers, T. P., Schwede, D. B., Hebert, E. O., and Neal, J. A.: Ozone and sulfur dioxide dry deposition to forests: Observations and model evaluation, J. Geophys. Res. Atmos., 105, 15 365–15 377, 2000.

Fowler, D., Flechard, C., Storeton-West, R. L., Sutton, M. A., Hargreaves, K. J., and Smith, R. I.: Long term measurements of SO2 dry deposition over vegetation and soil and comparisons with models, in: Studies in Environmental Science, edited by Erisman, G. J. H. a. J. W., vol. 64 of *Acid Rain Research: Do we have enough answers?Proceedings of a Specialty Conference*, pp. 9–19, Elsevier, 1995.

Garland, J. A., Atkins, D. H. F., Readings, C. J., and Caughey, S. J.: Deposition of gaseous sulphur dioxide to the ground, Atmos. Environ., 8, 75–79, 1974.

Granat, L. and Richter, A.: Dry deposition to pine of sulphur dioxide and ozone at low concentration, Atmos. Environ., 29, 1677–1683, 1995.

Hicks, B. B.: Dry deposition to forests—On the use of data from clearings, Agric. For. Meteorol., 136, 214–221, doi:10.1016/j.agrformet.2004.06.013, URL http://www.sciencedirect.com/science/article/pii/S0168192305002066, 2006.

Hicks, B. B., Baldocchi, D. D., Meyers, T. P., Hosker, R. P., and Matt, D. R.: A preliminary multiple resistance routine for deriving dry deposition velocities from measured quantities, Water, Air, & Soil Pollution, 36, 311–330, 1987.

Jensen, N. O. and Hummelshøj, P.: Erratum, Agric. For. Meteorol., 85, 289, doi:10.1016/S0168-1923(97)00024-5, URL http://www.sciencedirect.com/science/article/pii/S0168192397000245, 1997.

Matsuda, K., Watanabe, I., Wingpud, V., Theramongkol, P., and Ohizumi, T.: Deposition velocity of O_3 and SO_2 in the dry and wet season above a tropical forest in northern Thailand, Atmos. Environ., 40, 7557–7564, 2006.

Matt, D. R., McMillen, R. T., Womack, J. D., and Hicks, B. B.: A comparison of estimated and measured SO2 deposition velocities, Water. Air. Soil Pollut., 36, 331–347, doi:10.1007/BF00229676, URL http://link.springer.com.ezproxy.princeton.edu/article/10.1007/BF00229676, 1987.

Meyers, T., Finkelstein, P., Clarke, J., Ellestad, T., and Sims, P.: A multilayer model for inferring dry deposition using standard meteorological measurements, Journal of Geophysical Research-Atmospheres, 103, 22 645–22 661, 1998.

Meyers, T. P., Huebert, B. J., and Hicks, B. B.: HNO_3 deposition to a deciduous forest, Boundary Layer Meteorol., 49, 395–410, 1989.

Myles, L., Heuer, M. W., Meyers, T. P., and Hoyett, Z. J.: A comparison of observed and parameterized SO_2 dry deposition over a grassy clearing in Duke Forest, Atmos. Environ., 49, 212–218, 2012.

Neirynck, J., Flechard, C. R., and Fowler, D.: Long-term (13 years) measurements of SO_2 fluxes over a forest and their control by surface chemistry, Agric. For. Meteorol., 151, 1768–1780, 2011.

Nguyen, T. B., Crounse, J. D., Teng, A. P., Clair, J. M. S., Paulot, F., Wolfe, G. M., and Wennberg, P. O.: Rapid deposition of oxidized biogenic compounds to a temperate forest, Proc. Natl. Acad. Sci. U.S.A., 112, E392–E401, doi:10.1073/pnas.1418702112, URL http://www.pnas.org/content/112/5/E392, 2015.

Padro, J.: Observed characteristics of the dry deposition velocity of O3 and SO2 above a wet deciduous forest, Science of The Total Environment, 146-147, 395–400, doi:10.1016/0048-9697(94)90261-5, URL https://doi.org/10.1016/0048-9697(94)90261-5, 1994.

Padro, J., Neumann, H. H., and Hartog, G. D.: Dry deposition velocity estimates of SO_2 from models and measurements over a deciduous forest in winter, Water Air Soil Pollut., 68, 325–339, 1993.

Petroff, A. and Zhang, L.: Development and validation of a size-resolved particle dry deposition scheme for application in aerosol transport models, Geosci. Model Dev., 3, 753–769, 2010.

Pryor, S. C. and Klemm, O.: Experimentally derived estimates of nitric acid dry deposition velocity and viscous sub-layer resistance at a conifer forest, Atmos. Environ., 38, 2769–2777, 2004.

Sievering, H., Kelly, T., McConville, G., Seibold, C., and Turnipseed, A.: Nitric acid dry deposition to conifer forests:: Niwot Ridge spruce–fir–pine study, Atmos. Environ., 35, 3851–3859, doi:10.1016/S1352-2310(01)00156-X, URL http://www.sciencedirect.com/science/article/pii/S135223100100156X, 2001.

Sorimachi, A., Sakamoto, K., Ishihara, H., Fukuyama, T., Utiyama, M., Liu, H., Wang, W., Tang, D., Dong, X., and Quan, H.: Measurements of sulfur dioxide and ozone dry deposition over short vegetation in northern China—a preliminary study, Atmos. Environ., 37, 3157–3166, 2003.

Tsai, J.-L., Chen, C.-L., Tsuang, B.-J., Kuo, P.-H., Tseng, K.-H., Hsu, T.-F., Sheu, B.-H., Liu, C.-P., and Hsueh, M.-T.: Observation of SO2 dry deposition velocity at a high elevation flux tower over an evergreen broadleaf forest in Central Taiwan, Atmos. Environ., 44, 1011–1019, 2010.

Wesely, M. . L.: Parameterization of surface resistances to gaseous dry deposition in regional-scale numerical models, Atmos. Environ., 23, 1293–1304, 1989.

Wu, Z., Wang, X., Turnipseed, A. A., Chen, F., Zhang, L., Guenther, A. B., Karl, T., Huey, L. G., Niyogi, D., Xia, B., and Alapaty, K.: Evaluation and improvements of two community models in simulating dry deposition velocities for peroxyacetyl nitrate (PAN) over a coniferous forest, J. Geophys. Res. Atmos., 117, D04 310, 2012.

Wu, Z., Staebler, R., Vet, R., and Zhang, L.: Dry deposition of O_3 and SO_2 estimated from gradient measurements above a temperate mixed forest, Environ. Pollut., 210, 202–210, doi:10.1016/j.envpol.2015.11.052, URL http://www.sciencedirect.com/science/article/pii/S0269749115302128, 2016.

Zhang, L., Brook, J. R., and Vet, R.: A revised parameterization for gaseous dry deposition in air-quality models, Atmos. Chem. Phys., 3, 2067–2082, 2003.

Zhang, L., Jacob, D. J., Knipping, E. M., Kumar, N., Munger, J. W., Carouge, C. C., van Donkelaar, A., Wang, Y. X., and Chen, D.: Nitrogen deposition to the United States: distribution, sources, and processes, Atmos. Chem. Phys., 12, 4539–4554, 2012.